DALTON

Synthesis, electrochemistry and photophysics of ruthenium(II) diimine complexes of 1,1′-bis(diphenylphosphino)ferrocene (dppf). Crystal structure of $[Ru(bipy)_2(dppf)]^{2+}$ (bipy = 2,2′-bipyridine)†

Vivian Wing-Wah Yam,* Vicky Wing-Man Lee and Kung-Kai Cheung

Department of Chemistry, The University of Hong Kong, Pokfulam Road, Hong Kong

A series of ruthenium(II) diimine complexes of 1,1′-bis(diphenylphosphino)ferrocene (dppf), $[Ru(L-L)_2(dppf)]^{2+}$ [L–L = 2,2′-bipyridine (bipy), 4,4′-dimethyl-2,2′-bipyridine, 4,4′-di-*tert*-butyl-2,2′-bipyridine, or 1,10-phenanthroline] have been synthesized and their photophysical properties studied. The crystal structure of $[Ru(bipy)_2(dppf)]^{2+}$ has been determined. These complexes have been shown to exhibit low-energy emission at *ca.* 550 nm at 77 K, attributed to a $d_\pi(Ru) \longrightarrow \pi^*(L-L)$ metal-to-ligand charge transfer triplet excited state. The spectroscopic changes upon oxidation suggest it to occur on the ferrocene moiety.

The intriguing photophysical and photochemical properties of ruthenium(II) polypyridine complexes have rendered this class of complexes attractive to study, in particular their abilities to exhibit properties of importance to redox electrocatalysis and solar-energy conversion.[1,2] Recent developments have been extended towards the design and synthesis of chromophore-electroactive quencher systems in which electron acceptors such as 4,4′-bipyridinium, and/or donors such as phenothiazine, are covalently attached to the chromophore, $[Ru(bipy)_3]^{2+}$ (bipy = 2,2′-bipyridine).[3] The ferrocene moiety, being a redox-active electron-donor component, appears to be an attractive candidate for incorporation into the ruthenium(II) polypyridine system. Although there have been reports[4,5] on such introduction, focus was placed on the synthetic and electrochemical aspects with less attention being paid to the spectroscopic properties.

In this paper a series of ruthenium(II) polypyridine complexes containing the ferrocene moiety have been synthesized through the attachment of 1,1′-bis(diphenylphosphino)ferrocene (dppf). The spectroscopic, photophysical and electrochemical properties have been studied. In addition, the tuning of the spectroscopic properties of the complexes through a change in the oxidation state of the pendant ferrocenyl ligand and variation of the spectator ligands have also been investigated.

Experimental

2,2′-Bipyridine and 1,10-phenanthroline (phen) were obtained from Aldrich Chemical Company, 1,1′-bis(diphenylphosphino)ferrocene from Strem Chemicals Inc. The compounds 4,4′-dimethyl-2,2′-bipyridine (dmbipy), 4,4′-di-*tert*-butyl-2,2′-bipyridine (dbbipy) and the precursor complexes were prepared according to literature methods.[6] All solvents were purified and distilled by standard procedures before use. All other reagents were of analytical grade and used as received.

Synthesis of ruthenium(II) complexes

$[Ru(bipy)_2(dppf)][PF_6]_2$ 1. A mixture of *cis*-$[Ru(bipy)_2Cl_2]\cdot 2H_2O$ (131 mg, 0.25 mmol) and AgO_3SCF_3 (104 mg, 0.50 mmol) was stirred in acetone (15 cm^3) under nitrogen for 3 h. The mixture was then filtered to remove the precipitated AgCl and the filtrate added to a suspension of dppf (277 mg, 0.50 mmol) in acetone (15 cm^3). The mixture was then brought to reflux for 24 h, after which the resultant clear light orange solution was evaporated to dryness, extracted with MeOH–water (1:1 v/v) and then filtered to remove any unchanged reactants. Addition of a saturated solution of NH_4PF_6 afforded an orange solid. Slow diffusion of diethyl ether into an acetonitrile solution of the complex afforded **1** as orange crystals. Yield: 250 mg, 85%. ^1H NMR [300 MHz, $(CD_3)_2CO$, 298 K]: δ 9.57 (d, 2 H, *J* 5.6, bipy), 8.49 (d, 2 H, *J* 8.1, bipy), 8.27 (d, 2 H, *J* 7, bipy), 8.11–8.20 (m, 4 H, bipy), 7.69–7.76 (m, 4 H, bipy), 7.47 (t, 4 H, *J* 7 Hz, Ph), 7.32 (m, 2 H, bipy; 4 H, Ph), 7.06–7.26 (m, 8 H, Ph), 6.90 (m, 4 H, Ph), 5.31 (s, 2 H, C_5H_4), 4.94 (s, 2 H, C_5H_4), 4.65 (s, 2 H, C_5H_4) and 4.39 (s, 2 H, C_5H_4). Positive-ion fast atom bombardment (FAB) mass spectrum: *m/z* 1112, $[M + PF]^+$; 965 M^+ and 812 $[M - bipy]^+$ (Found: C, 51.4; H, 3.4; N, 4.2. Calc. for $C_{54}H_{44}F_{12}FeN_4P_4Ru$: C, 51.5; H, 3.5; N, 4.45%).

$[Ru(dmbipy)_2(dppf)][PF_6]_2$ 2. The procedure was similar to that for complex **1** except that $[Ru(dmbipy)_2Cl_2]$ (138 mg, 0.25 mmol) was used instead of $[Ru(bipy)_2Cl_2]\cdot 2H_2O$ to give orange crystals of **2**. Yield: 273 mg, 85%. ^1H NMR [300 MHz, $(CD_3)_2CO$, 298 K]: δ 9.04 (d, 2 H, *J* 6 Hz, bipy), 7.85 (s, 2 H, bipy), 7.62 (s, 2 H, bipy), 7.22–7.41 (m, 6 H, bipy; 8 H, Ph), 7.20–6.99 (m, 8 H, Ph), 6.73 (m, 4 H, Ph), 4.87 (s, 2 H, C_5H_4), 4.84 (s, 2 H, C_5H_4), 4.55 (s, 2 H, C_5H_4), 4.33 (s, 2 H, C_5H_4), 2.54 (s, 6 H, CH_3) and 2.46 (s, 6 H, CH_3). Positive-ion FAB mass spectrum: *m/z* 1023, M^+; 512, M^{2+} and 840, $[M - dmbipy]^+$ (Found: C, 57.05; H, 4.35; N, 4.35. Calc. for $C_{56}H_{48}Cl_2FeN_4O_8P_2Ru$: C, 56.95; H, 4.3; N, 4.6%).

$[Ru(dbbipy)_2(dppf)][PF_6]_2$ 3. The procedure was similar to that for compound **1** except that $[Ru(dbbipy)_2Cl_2]$ (159 mg, 0.25 mmol) was used instead of $[Ru(bipy)_2Cl_2]\cdot 2H_2O$ to yield orange crystals of **3**. Yield: 296 mg, 80%. ^1H NMR [300 MHz, $(CD_3)_2CO$, 298 K]: δ 9.49 (d, 2 H, *J* 6.1, bipy), 8.49 (d, 2 H, *J* 1.7, bipy), 8.38 (d, 2 H, *J* 2.2, bipy), 7.82 (dd, 2 H, *J* 2.2, 6.1, bipy), 7.48 (t, 2 H, *J* 7.3, Ph), 7.25–7.41 (m, 4 H bipy; 6 H, Ph), 7.13 (t, 4 H, *J* 7.3 Hz, Ph), 7.02 (m, 4 H, Ph), 6.95 (m, 4 H, Ph), 5.31 (s, 2 H, C_5H_4), 4.88 (s, 2 H, C_5H_4), 4.59 (s, 2 H, C_5H_4), 4.03 (s, 2 H, C_5H_4), 1.43 (s, 18 H, Bu^t) and 1.31 (s, 18 H, Bu^t). Positive-ion FAB mass spectrum: *m/z* 1338, $[M + PF_6]^+$; 1192, M^+; 597, M^{2+} and 926 $[M - dbbipy]^+$ (Found: C, 57.0; H, 5.15; N, 4.35. Calc for $C_{62}H_{60}F_{12}FeN_4P_4Ru\cdot CH_3CN$: C, 56.75; H, 5.25; N, 4.6%).

$[Ru(phen)_2(dppf)][PF_6]_2$ 4. The procedure was similar to that for complex **1** except that $[Ru(phen)_2Cl_2]$ (134 mg, 0.25 mmol) was used instead of $[Ru(bipy)_2Cl_2]\cdot 2H_2O$ to yield orange crystals of **4**. Yield: 287 mg, 88%. ^1H NMR [300 MHz, $(CD_3)_2CO$, 298 K]: δ 10.07 (d, 2 H, *J* 5.7, phen), 8.79 (d, 2 H, *J* 8.3, phen), 8.70 (d, 2 H, *J* 8.5 Hz, phen), 8.09–8.23 (m, 8 H, phen), 7.58

---

† *Non-SI unit employed*: eV ≈ 1.6×10^{-19} J.

(m, 2 H, phen), 7.42 (m, 2 H, Ph), 7.27 (m, 8 H, Ph), 7.00 (m, 2 H, Ph), 6.74 (m, 4 H, Ph), 6.54 (m, 4 H, Ph), 5.43 (s, 2 H, C_5H_4), 4.96 (s, 2 H, C_5H_4), 4.68 (s, 2 H, C_5H_4) and 4.58 (s, 2 H, C_5H_4). Positive-ion FAB mass spectrum: *m/z* 1161, $[M + PF_6]^+$; 1016, M^+ and 836, $[M - \text{phen}]^+$ (Found: C, 57.15; H, 3.25; N, 4.75. Calc. for $C_{58}H_{44}F_{12}FeN_4P_4Ru$: C, 57.35; H, 3.65; N, 4.6%).

Physical measurements and instrumentation

The UV/VIS spectra were obtained on a Hewlett-Packard 8452A diode-array spectrophotometer, and steady-state excitation and emission spectra on a Spex Fluorolog 111 spectrofluorometer. Low-temperature (77 K) spectra were recorded by using an optical Dewar sample holder. Proton NMR spectra were recorded on a Bruker DPX-300 Fourier-transform spectrometer with chemical shifts reported relative to tetramethylsilane, positive-ion FAB mass spectra on a Finnigan MAT95 spectrometer. Elemental analysis of the new complexes were performed by Butterworth Laboratories Ltd.

Emission lifetime measurements for Stern–Volmer quenching studies were performed using a conventional laser system. The excitation source was the 355 nm output (third harmonic) of a Quanta-Ray Q-switched GCR-150-10 pulsed Nd-YAG laser. Luminescence decay signals were recorded on a Tektronix model TDS 620A digital oscilloscope and analysed using a program for exponential fits. All solutions for photophysical studies were prepared under vacuum in a round-bottomed flask (10 cm^3) equipped with a side-arm 1 cm fluorescence cuvette and sealed from the atmosphere with a Kontes quick-release Teflon stopper. Solutions were rigorously degassed with no fewer than four freeze–pump–thaw cycles.

Electrochemical measurements were carried out with a PAR model 175 universal programmer and 173 potentiostat. Cyclic voltammograms were recorded with a Kipp & Zonen BD90 X-Y recorded at scan rates 50–500 mV s^{-1}. The electrolytic cell used was a conventional two-compartment cell. The reference electrode was Ag–$AgNO_3$ (0.1 mol dm^{-3} in acetonitrile) with a Vycor glass interfacing the working electrode compartment. Studies were performed in a non-aqueous medium (0.1 mol dm^{-3} NBu_4PF_6 in acetonitrile) with a glassy carbon (Atomergic Chemetal V25) electrode or a 5 × 30 × 50 mm graphite plate as working electrode for cyclic voltammetry and controlled-potential electrolysis, respectively, and a piece of platinum gauze as counter electrode separated from the working electrode by a sintered-glass frit. The ferrocenium-ferrocene couple was used as the internal reference in non-aqueous media for the cyclic voltammetric measurement.

Crystallography

Crystals of complex **1** were obtained by slow diffusion of diethyl ether into an acetonitrile solution of **1**.

Crystal data. $[C_{54}H_{44}FeN_4P_2Ru]^{2+}2PF_6^-$, $M = 1257.77$, tetragonal, space group $I4_1cd$ (no. 110), $a = 17.244(3)$, $b = 17.244(3)$, $c = 34.491(4)$ Å, $U = 10\,256.1(1.0)$ Å^3, $Z = 8$, $D_c = 1.629$ g cm^{-3}, μ(Mo-Kα) = 7.78 cm^{-1}, $F(000) = 5072$, $T = 298$ K.

A crystal of dimensions 0.25 × 0.15 × 0.30 mm was used for data collection at 25 °C on a Nonius-Enraf CAD4 diffractometer with graphite-monochromated Mo-Kα radiation ($\lambda = 0.710\,73$ Å) using ω–2θ scans with ω-scan angle $(0.5 + 0.35 \tan\theta)^\circ$ at a scan speed of 1.18–8.28° min^{-1}. Intensity data (in the range of $2\theta_{max} = 45^\circ$; *h* 0–15, *k* 0–18, *l* 0–37; three standard reflections measured after every 2 h showed decay of 3.30%) were corrected for decay and for Lorentz-polarization effects, and empirical absorption corrections based on the ψ scan of four strong reflections (minimum and maximum transmission factors 0.905 and 1.000). Upon averaging the 4681 reflections, 463 of which were uniquely measured ($R_{int} = 0.048$), 1663 with $I > 3\sigma(I)$ were considered observed and used in the structural analysis. The space group was determined from systematic absences and the structure was solved by Patterson and Fourier methods and refinement by full-matrix least squares using the SDP Program[7] on a Micro VAX II computer. A crystallographic asymmetric unit of 61 atoms consists of half of the complex cation with the Ru and Fe atoms at special positions and one PF_6^- anion. All 39 non-H atoms were refined anisotropically. Twenty-two hydrogen atoms at calculated positions with isotropic thermal parameters equal to 1.3 times that of the attached C atoms were included in the least-squares calculations but not refined. Convergence for 343 variable parameters by least-squares refinement on F with $w = 4F_o^2/\sigma^2(F_o^2)$, where $\sigma^2(F_o^2) = [\sigma^2(I) + (0.040F_o^2)^2]$ for 1663 reflections having $I > 3\,\sigma(I)$ was reached at $R = 0.032$ and $R' = 0.040$ with a goodness of fit of 1.15; $(\Delta/\sigma)_{max} = 0.01$. The final Fourier-difference map was featureless, with maximum positive and negative peaks of 0.35 and 0.27 e Å^{-3}, respectively.

Atomic coordinates, thermal parameters, and bond lengths and angles have been deposited at the Cambridge Crystallographic Data Centre (CCDC). See Instructions for Authors, *J. Chem. Soc., Dalton Trans.*, 1997, Issue 1. Any request to the CCDC for this material should quote the full literature citation and the reference number 186/510.

Results and Discussion

The complexes $[Ru(L-L)_2(dppf)]^{2+}$ (L–L = bipy, dmbipy, dbbipy or phen) were synthesized by the reaction of dppf with the corresponding bis(acetone)ruthenium(II) diimine precursor under reflux condition, a typical synthetic method for the preparation of heteroleptic ruthenium(II) complexes $[Ru(L-L)_2L']^{2+}$ where L′ is a bidentate ligand.[8] All the newly synthesized complexes gave satisfactory elemental analyses and have been characterized by positive-ion FAB mass spectrometry and ^1H NMR spectroscopy. Complex **1** has also been characterized by X-ray crystallography.

The ^1H NMR spectrum of complex **1** shows resonances in the aromatic region which are assigned to protons of the bipyridyl units and the phenyl ring on the dppf ligand. The ferrocenyl protons show resonances in the region δ 4.4–5.5, appearing as four singlets. This is different from that observed in other related 1,1′-disubstituted ferrocene compounds where the ferrocenyl signals usually appear as two triplets corresponding to the AA′BB′ spin system with a coupling constant of *ca.* 2 Hz for an eclipsed arrangement of the C_5H_4 rings.[9] This is suggestive of a staggered arrangement for the two C_5H_4 rings in **1**, which has been confirmed by X-ray crystallographic studies. Similar findings have been reported for $[Re(CO)_3Cl(dppf)]$ with the C_5H_4 rings in a staggered conformation.[10]

A perspective drawing of the cation of complex **1** with the atomic numbering is depicted in Fig. 1. Selected bond distances and angles are listed in Table 1. The complex adopts a distorted

Table 1 Selected bond lengths (Å) and angles (°) for complex **1** with estimated standard deviations in parentheses

Ru–P(1)	2.393(2)	P(1)–Ru–N(1)	96.9(1)
Ru–N(1)	2.103(5)	P(1)–Ru–N(2)	167.8(1)
Ru–N(2)	2.115(5)	N(1)–Ru–N(2)	77.5(2)
Fe–C(1)	2.023(6)	C(1)–Fe–C(2)	41.4(2)
P(1)–C(1)	1.831(6)	C(1)–Fe–C(3)	68.8(2)
P(1)–C(6)	1.851(6)	C(1)–Fe–C(4)	69.0(2)
P(1)–C(12)	1.840(6)	Ru–P(1)–C(1)	123.2(2)
N(1)–C(18)	1.328(8)	Ru–P(1)–C(6)	110.8(2)
N(1)–C(22)	1.363(8)	Ru–P(1)–C(12)	118.0(2)
N(2)–C(23)	1.340(8)	Ru–N(1)–C(18)	127.7(4)
N(2)–C(27)	1.350(8)	Ru–N(1)–C(22)	115.1(4)
C(1)–C(2)	1.441(8)	C(18)–N(1)–C(22)	117.2(6)
C(1)–C(5)	1.445(9)	Fe–C(1)–P(1)	130.3(4)
C(2)–C(3)	1.425(9)	Fe–C(1)–C(2)	70.3(3)
C(3)–C(4)	1.41(2)	P(1)–C(1)–C(2)	129.5(5)
C(4)–C(5)	1.424(9)	P(1)–C(1)–C(5)	122.7(4)

Table 2 Electrochemical and photophysical data for complexes **1**–**4**

Complex	$E_{\frac{1}{2}}$[a]/V *vs.* SCE Reduction	$E_{\frac{1}{2}}$[a]/V *vs.* SCE Oxidation	Absorption λ/nm (ε/dm^3 mol^{-1} cm^{-1})[b]	Emission λ/nm ($\tilde{\nu}_M$/cm^{-1})[c]
1	−1.30 −1.53	+0.91 (+1.83)	239 (sh) (50 205), 288 (27 040), 324 (sh) (10 815), 396 (6120)	544 (1325)
2	−1.39 −1.59	+0.90 (+1.80)	246 (sh) (39 235), 286 (29 150), 320 (sh) (11 355), 393 (6075)	537 (1425)
3	−1.43 −1.63	+0.91 (+1.80)	246 (sh) (40 940), 288 (32 670), 318 (sh) (13 900), 390 (7195)	573 (1355)
4	−1.28 (−1.48)	+0.90 (+1.91)	232 (sh) (72 965), 266 (41 255), 300 (sh) (18 500), 368 (8510), 410 (sh) (5955)	569 (1150)

[a] In acetonitrile solution with 0.1 mol dm^{-3} NBu$_4$PF$_6$ as supporting electrolyte at room temperature. Working electrode, glassy carbon; scan rate 100 mV s^{-1}. Values in parentheses correspond to peak potentials of irreversible waves. [b] In acetonitrile at 298 K. [c] In ethanol–methanol (4 : 1 v/v) glass at 77 K.

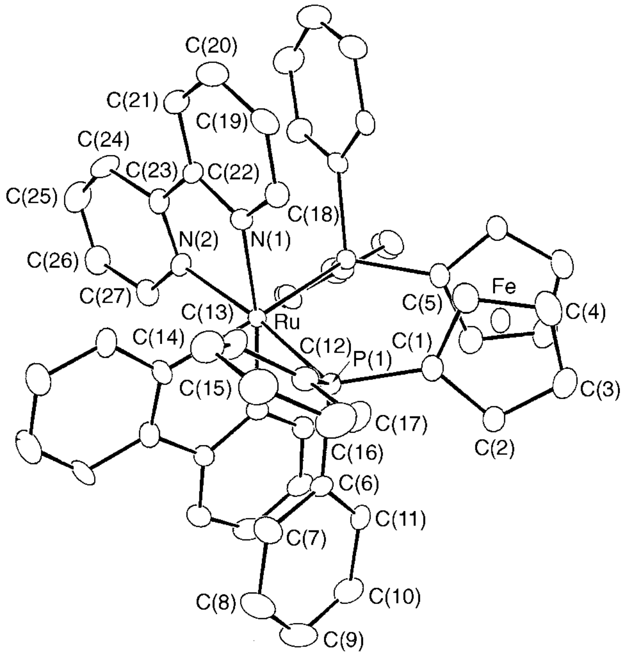

Fig. 1 Perspective drawing of the cation of complex **1** with the atomic numbering. The thermal ellipsoids are shown at the 40% probability level

octahedral geometry at Ru. The N–Ru–N bond angle subtended by the chelating bipyridine is 77.6°, much distorted from a regular octahedral geometry as a result of the steric requirement of bipyridine. The P–Ru–N angle of 96.9° is slightly larger than the ideal value of 90°. The cyclopentadienyl rings in the bidentate dppf ligand are staggered, with a deviation from the eclipsed conformation of 24.09°. A staggered conformation of the two cyclopentadienyl rings has also been reported in the square-planar complexes [Rh(nbd)(dppf)]$^+$ (nbd = norbornadiene = bicyclo[2.2.1]hepta-2,5-diene),[11] [PtCl$_2$(dppf)][12] and [PdCl$_2$(dppf)][13,14] and in the octahedral complexes [Re(CO)$_3$Cl(dppf)][10] and [Mo(CO)$_4$(dppf)],[14] while an eclipsed conformation of the rings was observed for the tetrahedral complexes of Ni[14] and Mn.[15] The cyclopentadienyl rings are planar but deviate slightly from being parallel with a dihedral angle of 1.58°. In addition, the P atoms are slightly displaced out of the plane by 0.186 Å away from the Fe atom. These conformational arrangements, ring tilt and P atom displacement are probably related to the steric requirements of the bonding to the Ru atom. Similar variations in geometry have been found in a series of related complexes of Rh, Pd, Ni and Mo.[11,14] The separation between Fe and Ru is 4.51 Å, too long for any significant metal–metal interaction to exist.

Electrochemical data for complexes **1**–**4** in acetonitrile are collected in Table 2. The cyclic voltammograms of all the complexes display a reversible oxidation couple at *ca.* +0.90 V *vs.* SCE, independent of scan rate, and with a ΔE_p of *ca.* 60 mV. Possible origins of this couple could be either a metal-centred Ru$^{3+/2+}$ couple or the dppf ligand-centred oxidation, localized on the redox-active ferrocene moiety. The relative insensitivity of the potential to the nature of the spectator ligand, together with the fact that Ru$^{3+/2+}$ couples for dicationic ruthenium(II) polypyridine complexes commonly occur in the range +1.20 to +1.75 V *vs.* SCE, suggest that the first oxidation is unlikely to be ruthenium(II) based but rather dppf based instead. The observation that this dppf-centred oxidation occurs at a more positive potential than that of free dppf, E_{pa} +0.27 V *vs.* ferrocenium–ferrocene,[10] is in line with its reduced ease of oxidation upon co-ordination to ruthenium(II). Upon scanning to a more positive potential a second oxidation process which is irreversible appears at *ca.* +1.80 V *vs.* SCE. This is tentatively suggested to be a result of the oxidation at the diphenylphosphine moiety to give a short-lived co-ordinated phosphenium cation.

$$[\mathrm{Ru^{II}(L{-}L)_2(dppf^{\bullet+})}]^{3+} + e^- \rightleftharpoons [\mathrm{Ru^{II}(L{-}L)_2(dppf)}]^{2+}$$

$$[\mathrm{Ru^{II}(L{-}L)_2(dppf)}]^{2+} + e^- \rightleftharpoons [\mathrm{Ru^{II}(L{-}L)(L{-}L^{\bullet-})(dppf)}]^{+}$$

$$[\mathrm{Ru^{II}(L{-}L)(L{-}L^{\bullet-})(dppf)}]^{+} + e^- \rightleftharpoons [\mathrm{Ru^{II}(L{-}L^{\bullet-})_2(dppf)}]$$

Scheme 1

The Ru$^{3+/2+}$ couple, which is commonly observed in the range +1.20 to +1.75 V *vs.* SCE for ruthenium(II) polypyridine dications, was not observed upon scanning to +1.80 V for the [Ru(L–L)$_2$(dppf)]$^{2+}$ complexes. The ruthenium(II)-based oxidation probably occurs at a more positive potential than those of homoleptic ruthenium(II) polypyridine complexes such as [Ru(bipy)$_3$]$^{2+}$ in view of the better π-acceptor ability of the phosphine ligand than those of ligands of the bipyridyl type. Thus the lower oxidation state ruthenium(II) would be more preferentially stabilized and a shift in the reduction potential to a more positive value would be observed. Furthermore, the prior oxidation of the dppf ligand would impose a higher overall positive charge on the complexes and render further oxidation of the complexes difficult. Thus it is likely that the metal-centred oxidation for [Ru(L–L)$_2$(dppf)]$^{2+}$ occurs at a potential more positive than that of [Ru(bipy)$_2$(Ph$_2$PCH$_2$PPH$_2$)]$^{2+}$ [+1.63 V *vs.* saturated sodium chloride electrode (SSCE)] and [Ru(bipy)$_2$(*cis*-Ph$_2$PCH=CHPPh$_2$)]$^{2+}$ (+1.75 V *vs.* SSCE),[8] and possibly so positive that it occurs beyond the solvent window for measurements. On the other hand, the reduction couples of the complexes correspond to sequential one-electron reductions of their diimine ligands. The reversible redox couples can be summarized as in Scheme 1.

The UV/VIS absorption spectral data for complexes **1**–**4** are summarized in Table 2. The electronic absorption spectrum is dominated by an intense band in the UV region and a medium band in the visible region. The band of **1** at *ca.* 288 nm in the UV region with a large absorption coefficient is tentatively assigned as a $\pi \longrightarrow \pi^*$ transition localized on either the bipyridine ligands or the phenyl groups. The band at *ca.* 400 nm with an absorption coefficient of 6210 dm^3 mol^{-1} cm^{-1} is assigned as the d_π(Ru) $\longrightarrow$ π^*(bipy) metal-to-ligand charge-transfer (m.l.c.t.) transition. Similar assignments have been reported for analogous mixed phosphine–bipyridine complexes of ruthenium(II).[8] It is likely that any dppf-centred absorption which has a very small absorption coefficient and usually occurs at a similar region for free dppf (ε_{420} = 210 dm^3 mol^{-1} cm^{-1}) would be masked by the intense m.l.c.t. band. The lower m.l.c.t. absorption energy of **1** than that of the related complexes $[Ru(bipy)_2(Ph_2PCH_2PPh_2)]^{2+}$ (384 nm) and $[Ru(bipy)_2$-$(cis$-$Ph_2PCH{=}CHPPh_2)]^{2+}$ (373 nm) is suggestive of a higher d_π(Ru) orbital energy in **1**, assuming the π^*(L–L) orbital energy remains relatively constant for the same bipyridine ligand as reflected by the almost identical $E_{\frac{1}{2}}$ values for the diimine-based reduction of all the three complexes. This finding is in line with the comparatively poorer π-acceptor ability of the dppf ligand expected with its ferrocenyl moiety being a good electron donor.

Excitation of degassed acetonitrile solutions of complexes **1**–**4** at room temperature did not result in emission characteristic of the m.l.c.t. triplet state. An appreciable emission can only be observed at low temperatures. The photophysical data are collected in Table 2. The results reveal that the complexes are higher-energy emitters at 77 K in alcohol glasses than is $[Ru(bipy)_3]^{2+}$. The emission spectra of the $[Ru(L\text{–}L)_2$-$(dppf)]^{2+}$ complexes all display well resolved vibronic bands with vibrational progressional spacings ($\tilde{\nu}_M$) ranging from 1150 to 1425 cm^{-1}. Emission spectra of this type are typical for m.l.c.t. excited states with diimines as the chromophoric ligands.[16] The vibrational progressions appear to be assignable to the ν(L–L) framework vibrations.

The observation of emissive properties upon lowering of temperature is commonly encountered in $[Ru(L\text{–}L)_2L'_2]^{2+}$ (L = phosphine) complexes.[16] The lack of luminescent properties of the $[Ru(L\text{–}L)_2L'_2]^{2+}$ complexes at room temperature can be rationalized by the enhanced rate of the m.l.c.t. to d–d transition state as a result of the π acidity of the phosphine ligands which destabilizes the lowest m.l.c.t. state to a far greater extent than the d–d state compared, for example, to that of the luminescent $[R(bipy)_3]^{2+}$.[16] The presence of the ferrocenyl moiety, which would be expected to act as both a good reductive quencher ($E_{\frac{1}{2}} \approx +0.377$ V *vs.* SCE) and an energy acceptor ($E_T \approx 1.65$ eV)[17] for ruthenium(II) polypyridine complexes, may also be another contributing factor to the non-emissive property observed at room temperature. The quenching of $[Ru(bipy)_3]^{2+}$ by dppf in acetonitrile solution (0.1 mol dm^{-3} NBu_4PF_6) shows that the dppf ligand can act as an efficient electron- and energy-transfer quencher for the ^{3}m.l.c.t. excited state of $[Ru(bipy)_3]^{2+}$ with a bimolecular quenching rate constant, k_q, of 1.3×10^9 dm^3 mol^{-1} s^{-1} $\{E°[Ru(bipy)_3{}^{2+*/+}] = +0.77$ V *vs.* SCE;[18] $E_{pa}(dppf^{+/0}) \approx +0.65$ V *vs.* SCE;[10] $E_{0\text{-}0}$-$[Ru(bipy)_3{}^{2+*/2+}] \approx 2.13$ eV$\}$.[18] It is therefore likely that coordination of dppf to the $Ru(bipy)_2$ unit would also quench the emission of the complexes through very efficient intramolecular electron- and energy-transfer quenching processes, given the $E°[Ru(bipy)_2(dppf)^{2+*/+}] = +0.98$ V *vs.* SCE and $E_{0\text{-}0}[Ru(bipy)_2(dppf)^{2+*/2+}] \approx 2.28$ eV estimated for complex **1**. Similar excited-state reduction potentials and zero–zero emission energies have been reported for the related $[Ru(bipy)_2(Ph_2PCH_2CH_2PPh_2)]^{2+}$ and $[Ru(bipy)_2(cis$-$Ph_2PCH{=}CHPPh_2)]^{2+}$ complexes.[16]

The UV/VIS spectral traces of complex **1** in acetonitrile (0.1 mol dm^{-3} NBu_4PF_6) during the course of controlled-potential electrolysis at a potential slightly more positive than the first oxidation couple show the generation of a broad absorption band at *ca.* 620 nm with an absorption coefficient of 565 dm^3 mol^{-1} cm^{-1}, characteristic of the ferrocenium ion (λ_{max} = 617 nm, ε = 450 dm^3 mol^{-1} cm^{-1}).[19] Similar observations have been reported for rhenium(I) dppf complexes.[10] On the other hand, controlled-potential electrolysis of other related ruthenium(II) phosphine complexes but without the ferrocene moiety was reported by Meyer and co-workers[8] to show UV/VIS spectral data typical of the oxidized ruthenium(III) species. The $[Ru^{III}(bipy)_2\{Ph_2P(CH_2)_3PPh_2\}]^{3+}$ and $[Ru^{III}(bipy)_2(cis$-$Ph_2PCH{=}CHPPh_2)]^{3+}$ species generated by controlled-potential oxidation of the respective $[Ru(bipy)_2\{Ph_2P(CH_2)_3PPh_2\}]^{2+}$ and $[Ru(bipy)_2(cis$-$Ph_2PCH{=}CHPPh_2)]^{2+}$ display absorption band at *ca.* 779 and 840 nm, respectively, assigned as ligand-to-metal charge-transfer (l.m.c.t.) transitions, while a band at *ca.* 385 nm has been assigned as either a π_b(bipy) $\longrightarrow$ $d_\pi(Ru^{III})$ l.m.c.t. or $d_\pi(Ru^{III})$ $\longrightarrow$ π^*(bipy) m.l.c.t. transition.[8] The occurrence of the absorption band at *ca.* 620 nm upon oxidation of **1**, which is of higher energy than those observed for $[Ru^{III}(bipy)_2\{Ph_2P(CH_2)_3PPh_2\}]^{3+}$ and $[Ru^{III}(bipy)_2(cis$-$Ph_2PCH{=}CHPPh_2)]^{3+}$ and typical of the ferrocenium ion, further supports the assignment of the first reversible oxidation to the ferrocene-centred one on the dppf ligand in the cyclic voltammetric studies.

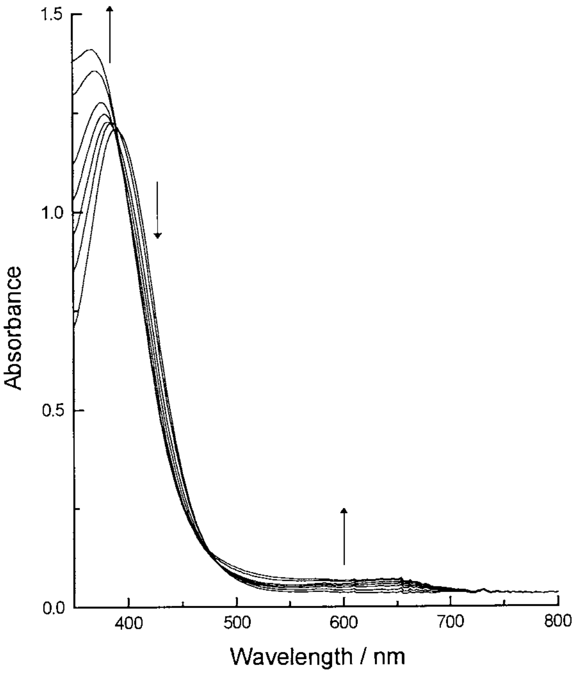

Fig. 2 The UV/VIS absorption spectral traces of complex **1** in acetonitrile upon oxidation with ammonium cerium(IV) nitrate

The UV/VIS spectral traces of complexes **1** and **3** upon titration with the oxidizing agent ammonium cerium(IV) nitrate in acetonitrile are shown in Figs. 2 and 3, respectively. Those of **1** upon chemical oxidation are similar to those obtained by controlled-potential electrolysis. A broad band at *ca.* 620 nm is generated and a shift of the m.l.c.t. absorption band at *ca.* 396 nm to higher energy at *ca.* 370 nm is observed, with two isosbestic points centred at 396 and 470 nm. The generation of the absorption band at *ca.* 620 nm with an absorption coefficient in the order of 10^2 dm^3 mol^{-1} cm^{-1} indicates formation of the ferrocenium ion. Fig. 4 shows the titration curve for the cerium(IV) titration of **1** in acetonitrile, which levels off after addition of about 1 mol equivalent of ammonium cerium(IV) nitrate, indicating that the redox reaction is a one-electron process as cerium(IV) is a one-electron oxidant. The reaction that is likely to proceed is $[Ru(L\text{–}L)_2(dppf)]^{2+} + Ce^{4+} \longrightarrow [Ru(L\text{–}L)_2$-$(dppf^{\bullet+})]^{3+} + Ce^{3+}$.

The blue shift in the d_π(Ru) $\longrightarrow$ π^*(L–L) m.l.c.t. absorption energy upon oxidation may be attributed to the electron-withdrawing nature of the bis(diphenylphosphino)ferrocenium cation, which would render the metal centre less electron rich and less readily able to donate its electron in the m.l.c.t. transition. The oxidation would also render the dppf ligand a better π acceptor and therefore the d_π orbitals of the ruthenium(II) centre would be more stabilized, leading to a lowering of the d_π orbital energies, and hence a shift in the $d_\pi(Ru^{II}) \longrightarrow \pi^*(L\text{–}L)$ m.l.c.t. transition to higher energy would occur.

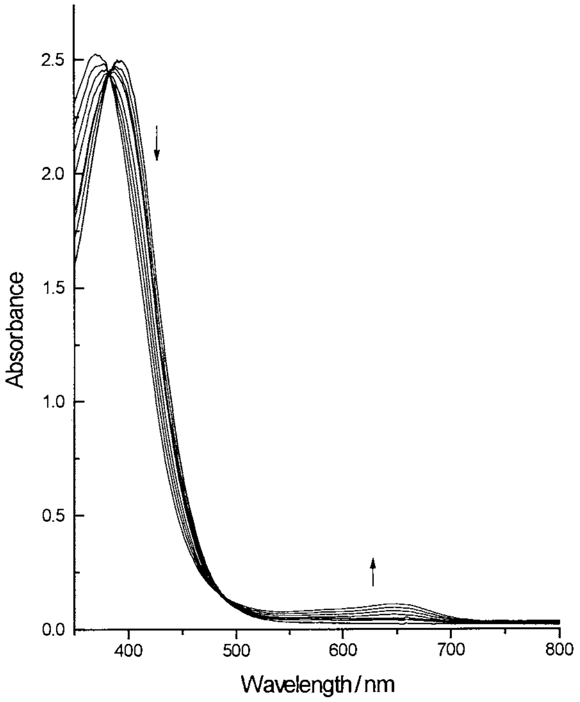

Fig. 3 The UV/VIS absorption spectral traces of complex **3** in acetonitrile at 298 K upon oxidation with ammonium cerium(IV) nitrate

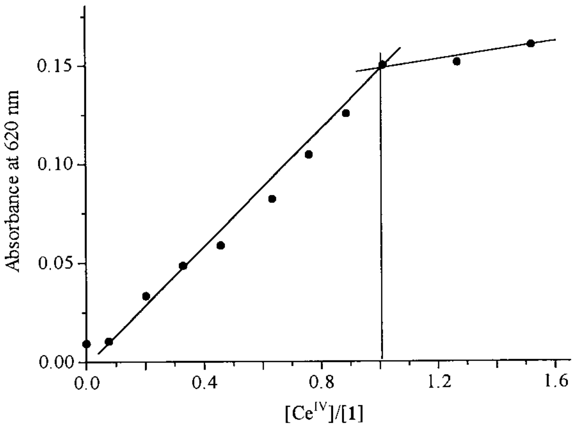

Fig. 4 Titration curve for the oxidation of complex **1** with ammonium cerium(IV) nitrate in acetonitrile

Acknowledgements

V. W.-W. Y. acknowledges financial support from the Research Grants Council and The University of Hong Kong. V. W.-M. L. acknowledges the receipt of a postgraduate studentship, administered by The University of Hong Kong.

References

1 T. J. Meyer, *Acc. Chem. Res.*, 1981, **22**, 163.
2 J. S. Connolly, *Photochemical Conversion and Storage of Solar Energy*, Academic Press, New York, 1981.
3 E. Danielson, C. M. Elliott, J. W. Merkert and T. J. Meyer, *J. Chem. Soc., Chem. Commun.*, 1994, 2075.
4 P. D. Beer and O. Kocian, *J. Chem. Soc., Dalton Trans.*, 1990, 3283.
5 I. R. Butler, *Organometallics*, 1992, **11**, 74.
6 W. H. F. Sasse, *Org. Synth.*, 1973, Coll. Vol. **V**, 102.
7 SDP, Structure Determination Package, Enraf-Nonius, Delft, 1985.
8 B. P. Sullivan, D. J. Salmon and T. J. Meyer, *Inorg. Chem.*, 1978, **17**, 3334.
9 R. Broussier, A. Da Rold, B. Gautheron, Y. Dromzee and Y. Jeannin, *Inorg. Chem.*, 1990, **29**, 1817.
10 M. M. Timothy, J. A. Kazi and M. S. Wrighton, *Inorg. Chem.*, 1989, **28**, 2347.
11 W. R. Cullen, T. J. Kim, F. W. B. Einstein and T. Jones, *Organometallics*, 1983, **2**, 714.
12 D. A. Clemente and G. Pilloni, *Inorg. Chim. Acta*, 1986, **115**, L9.
13 T. Hayashi, M. Konishi, M. Kobori, M. Kumada, T. Higuchi and K. Hirotsu, *J. Am. Chem. Soc.*, 1984, **106**, 158.
14 I. R. Butler, W. R. Cullen, T.-J. Kim, S. J. Rettig and J. Trotter, *Organometallics*, 1985, **4**, 972.
15 S. Onaka, *Bull. Chem. Soc. Jpn.*, 1986, **59**, 2359.
16 J. V. Caspar and T. J. Meyer, *Inorg. Chem.*, 1983, **22**, 2444.
17 W. G. Herkstroeter, *J. Am. Chem. Soc.*, 1975, **97**, 4161.
18 C. R. Bock, J. A. Connor, A. R. Gutierrez, T. J. Meyer, D. G. Whitten, B. P. Sullivan and J. K. Nagle, *J. Am. Chem. Soc.*, 1979, **101**, 4815.
19 Y. S. Sohn, D. N. Hendrickson and H. B. Gray, *J. Am. Chem. Soc.*, 1971, **93**, 3603.

Received 21*st November* 1996; *Paper* 6/07923G